

A positivity-preserving finite element method for chemotaxis problems in 3D

Robert Strehl* Andriy Sokolov* Dmitri Kuzmin[†]
Dirk Horstmann[‡] Stefan Turek*

December 17, 2010

Abstract

We present an implicit finite element method for a class of chemotaxis models in three spatial dimensions. The proposed algorithm is designed to maintain mass conservation and to guarantee positivity of the cell density. To enforce the discrete maximum principle, the standard Galerkin discretization is constrained using a local extremum diminishing flux limiter. To demonstrate the efficiency and robustness of this approach, we solve blow-up problems in a 3D chemostat domain. To give a flavor of more complex and realistic chemotactic applications, we investigate the pattern dynamics and aggregating behavior of the bacteria *Escherichia coli* and *Salmonella typhimurium*. The obtained numerical results are in good qualitative agreement with theoretical studies and experimental data reported in the literature.

Key words: chemotaxis models, flux limiters, finite elements, pattern formation, bacteria aggregation

*Institut für Angewandte Mathematik, TU Dortmund, E-mail addresses: robert.strehl@math.uni-dortmund.de, asokolow@math.uni-dortmund.de, ture@featflow.de.

[†]Universität Erlangen-Nürnberg, E-mail address: kuzmin@am.uni-erlangen.de.

[‡]Mathematisches Institut der Universität zu Köln, E-mail address: dhorst@math.uni-koeln.de.

1 Introduction

Chemotaxis, an oriented movement towards or away from regions of higher concentrations of chemical species, plays a vitally important role in the evolution of many living organisms. Experimental studies confirm that certain species (cells or bacteria) experience collective motion driven by attraction to or repulsion by other species (medicine, food, tumor angiogenic factor) [12]. The simplest mathematical description of chemotactic cell motion was proposed by Patlak [56], Keller and Segel [40, 41]. Various extensions of their models have been used to analyze tumor angiogenesis and invasion [15, 8], vasculogenesis [7], mesenchymal motion [31, 16], biological pattern formation [3, 67], multi-species chemotaxis with attraction and repulsion between competitive interacting species [35, 34] etc.

From the mathematical point of view, several interesting questions arise in the context of classical (also called *minimal*) chemotaxis models. In particular, unbounded aggregation of cells may give rise to singularities at accumulation points. This phenomenon is known as the *blow-up* effect. Theoretical studies have shown that solutions to the 1D minimal model cannot blow up (see, e.g., [55]). In two dimensions, the existence of blow-up solutions depends on the initial cell density u_0 and chemotactic sensitivity χ . It is known that a (bounded) solution exists globally in time if $\|u_0\|_{L^1(\Omega)} < 4\pi\chi^{-1}$ in the nonsymmetric case and $\|u_0\|_{L^1(\Omega)} < 8\pi\chi^{-1}$ in the presence of radial symmetry [36]. Otherwise, a blow-up occurs in finite time whenever $\int_{\Omega} |\mathbf{x} - \mathbf{x}_0|^2 u_0(\mathbf{x}) d\mathbf{x} \ll 1$ for some $\mathbf{x}_0 \in \Omega$. For details, we refer to Nagai [52], Senba & Suzuki [62], and Horstmann & Wang [37].

In three dimensions, the threshold for the blow-up effect may also depend on the initial cell density, on the form of the chemotactic sensitivity, and on other parameters (see, e.g., [21, 20]). Perthame [57] showed that there is a blow-up in finite time if $(\int_{\Omega} |x|^2 u_0(\mathbf{x}) d\mathbf{x})^2 < C\|u_0\|_{L^1(\Omega)}^2$, where C is a small constant. Horstmann and Winkler [38] studied conditions under which the solution of a chemotaxis system with a chemotactic sensitivity of the form $\chi = cu^\alpha$ (where c and α are some constants) remains bounded or blows up in finite or infinite time. Their results prove the existence of initial data that give rise to blow-up solutions of the classical chemotaxis model in a bounded domain $\Omega \subset \mathbb{R}^3$. The existence, uniqueness, and uniform-in-time boundedness of global classical solutions for a 3D chemotaxis-haptotaxis system were investigated by Tao and Wang [65].

Another interesting phenomenon is the fact that a homogeneous stationary solution may become unstable for large values of the sensitivity function $\chi(u)$ under

some conditions on the reactive source term in the chemotactic growth system. Such instabilities may give rise to rapidly evolving transient solutions, forming patterns which are observed in biological experiments (see, e.g., [4, 3, 64]).

The wealth of the methods for the numerical solution of chemotaxis problems includes positivity-preserving finite volume and finite element schemes [17, 25, 60], fractional step algorithms based on operator splitting [59, 69], interior penalty / discontinuous Galerkin methods [23, 24], and cell-overcrowding prevention models [13, 22, 58]. However, special care is required when it comes to the numerical simulation of the blow-up phenomenon and pattern formation. Steep gradients, spikes, and propagating fronts may give rise to nonphysical oscillations if the numerical scheme is not guaranteed to satisfy the discrete maximum principle (DMP). As a result, the cell density may become negative. Moreover, the blow-up or instability of approximate solutions may occur for purely numerical reasons.

In the present paper, we employ a high-resolution finite element scheme which satisfies the discrete maximum principle for linear and multilinear approximations on unstructured meshes. This algorithm is labeled FEM-TVD since it is based on a multidimensional generalization of total variation diminishing schemes for 1D conservation laws [43, 44]. The proposed methodology guarantees mass conservation and keeps the cell density nonnegative. Another objective of this paper is to perform a series of numerical experiments for chemotaxis problems in the three-dimensional case. Most numerical studies published to date are concerned with 2D simulations, whereas the numerical behavior of solutions in 3D remains largely unexplored.

The article is organized as follows. In section 2, we provide the analytical background and theoretical results for chemotaxis models in 3D. In section 3, we outline the FEM-TVD algorithm that we used in the numerical study to be presented in section 4. We demonstrate that the FEM-TVD method is well-suited for numerical simulations of chemotaxis problems, even in situations when the pure Galerkin method fails. In subsections 4.2 and 4.3, we consider realistic chemotaxis models which describe the aggregation and proliferation of the bacteria *Escherichia coli* and *Salmonella typhimurium*. Section 5 summarizes the pros and cons of the proposed approach.

2 Analytical background and theoretical results for chemotaxis models in 3D

The generic form of the chemotaxis problem to be solved in a three-dimensional domain $\Omega \subset \mathbb{R}^3$ reads

$$u_t = \nabla \cdot (D(u)\nabla u - A(u)B(c)C(\nabla c)) + q(u) \quad \text{in } \Omega, \quad (1)$$

$$c_t = d\Delta c - s(u)c + g(u)u \quad \text{in } \Omega, \quad (2)$$

where $u(t, \mathbf{x})$ denotes the cell density and $c(t, \mathbf{x})$ is the chemoattractant concentration. A particular model is defined by the formulae for the generic coefficients $D(\cdot)$, $A(\cdot)$, $B(\cdot)$, $C(\cdot)$, $q(\cdot)$, d , $s(\cdot)$, $g(\cdot)$. The above transport equation for u and reaction-diffusion equation for c are endowed with the initial conditions

$$u|_{t=0} = u_0, \quad c|_{t=0} = c_0 \quad \text{in } \Omega. \quad (3)$$

It is common to prescribe the homogeneous Neumann boundary conditions

$$\mathbf{n} \cdot \nabla u = 0 \quad \mathbf{n} \cdot \nabla c = 0 \quad \text{on } \Gamma, \quad (4)$$

or total flux boundary conditions of the form

$$\mathbf{n} \cdot (D(u)\nabla u - A(u)B(c)C(\nabla c)) = 0, \quad \mathbf{n} \cdot \nabla c = 0 \quad \text{on } \Gamma, \quad (5)$$

where \mathbf{n} is an outward normal to the boundary $\Gamma = \partial\Omega$.

Before presenting a brief summary of the theoretical results for the above class of chemotaxis models, we cite a local existence result for the following problem

$$\left. \begin{aligned} u_t &= \nabla \cdot (\nabla u - \chi(u, c)\nabla c) + f(u, c), & \mathbf{x} \in \Omega, t > 0 \\ \tau c_t &= \Delta c + g(u, c), & \mathbf{x} \in \Omega, t > 0 \\ \mathbf{n} \cdot \nabla u &= \mathbf{n} \cdot \nabla c = 0, & \mathbf{x} \in \Gamma, t > 0 \\ u(0, \mathbf{x}) &= u_0(\mathbf{x}), c(0, \mathbf{x}) = c_0(\mathbf{x}), & \mathbf{x} \in \Omega. \end{aligned} \right\} \quad (6)$$

Theorem 2.1 (compare Theorem 7.2 in [63]) *Suppose that $\Omega \subset \mathbb{R}^N$ is a convex domain with smooth boundary $\partial\Omega$, $\tau > 0$, and χ , f and g are smooth functions of u and c . Let u_0 and c_0 be in $C^{4,\theta}(\Omega)$ for $\theta \in (0, 1)$. If the compatibility conditions are satisfied on the boundary, then there exists a unique classical solution (u, c) to (6) in Q_T for some $T > 0$. Moreover, u and c are in $C^{2,\theta}(Q_T)$.*

Of course, there exist other results on the local existence of solutions to general chemotaxis equations. Moreover, one can also derive some alternative versions, for example, by applying the theorems of H. Amann [5, 6] and A. Yagi [71]. However, the theorem above is sufficient for our purposes.

In this paper we concentrate on three model problems. In particular, we consider the following chemotaxis models

$$\text{classical:} \quad \begin{cases} u_t = \Delta u - \chi \nabla \cdot (u \nabla c), \\ c_t = \Delta c - c + u, \end{cases} \quad (7)$$

$$\text{pattern formation:} \quad \begin{cases} u_t = d_u \Delta u - \chi \nabla \cdot (u \nabla c) + u(1 - u), \\ c_t = \Delta c - \beta c + u, \end{cases} \quad (8)$$

$$\text{aggregation:} \quad \begin{cases} u_t = d_u \Delta u - \chi \nabla \cdot \left[\frac{u}{(1+c)^2} \nabla c \right], \\ c_t = \Delta c - c + w \frac{u^2}{\mu + u^2}. \end{cases} \quad (9)$$

There is a crucial difference between model (7) and models (8) and (9). The reactive term $u(1 - u)$ in system (8) prevents its solution from blowing up in a finite time (see for instance [66]). The blow-up is also impossible for the third model (which can be shown quite easily by applying Alikakos' method of the Moser iteration and standard regularity result for abstract evolution equations, see [32, Theorem 4 and Remark 3]). However, the first model does allow the finite time blow-up phenomenon, and its study has attracted the attention of many scientists. The first step in understanding the possibility of finite time blow-up for the first model has been made by V. Nanjundiah [54], who performed a non-linear stability analysis in space dimension $N = 2$. His studies result in the conclusion that:

“The end-point (in time) of the aggregation is such that the cells are distributed in the form of δ -function concentrations.”

Nanjundiah's paper was followed by the papers by S. Childress and J. K. Percus that contain the famous conjectures regarding the asymptotic behavior of the solution of the Keller-Segel model for the space dimensions $N = 1$, $N = 2$, and $N \geq 3$. This conjecture says the following (see [19, page 236-237]):

“In particular, for the special model we have investigated, collapse cannot occur in a one-dimensional space; may or may not in two dimensions, depending upon the cell population; and must, we surmise, in three or more dimensions under a perturbation of sufficiently high symmetry.”

Childress and Percus refer to aggregation that proceeds to the formation of δ -functions in the cell density as *chemotactic collapse*. For the one- and two-dimensional results, we refer to [33] and the references therein. Surprisingly enough, little attention has been paid so far to the three-dimensional case. In spite of its practical importance, it was analyzed rather superficially compared to the one- and two-dimensional situations. However, the following results are known for the three-dimensional version of the parabolic-elliptic PDE system (7).

Suppose that $\Omega \subset \mathbb{R}^3$ is a ball or the space \mathbb{R}^3 itself. Then there exist initial data such that the corresponding solution blows up in finite time, see [51, 29, 30, 28]. The case of $\Omega = \mathbb{R}^3$ was investigated in [29, 30, 28]. It was shown that for any $T > 0$ and any constant $C > 0$ there exists a radial solution $(u(t, r), c(t, r))$ to a parabolic-elliptic version of system (7). This solution is smooth for all times $0 < t < T$, blows up at $r = 0$ and $t = T$, and has the property

$$\int_{|x| \leq r} u(T, s) ds \rightarrow C.$$

For any $T > 0$ there exists a sequence $\{\delta_n\}_{n \in \mathbb{N}}$ with $\lim_{n \rightarrow \infty} \delta_n = 0$, and a sequence of radial solutions $(u_n(t, r), c_n(t, r))$ that blow up at $r = 0$ and $t = T$, and are such that $u_n(t, r)$ is self-similar. Furthermore,

$$u_n(t, r) \sim \left(\frac{8\pi}{\chi} + \delta_n \right) (4\pi r^2)^{-1} \text{ as } r \rightarrow 0.$$

For this solution

$$\int_{|x| \leq r} u(T, s) ds \rightarrow 0 \text{ as } r \rightarrow 0.$$

Corrias, Perthame and Zaag [21] showed that Childress’ and Percus’ conjecture does not hold for $\Omega = \mathbb{R}^N$ ($N \geq 3$). In this particular case, they proved the existence of initial data such that weak solutions of the parabolic-elliptic case of (7) exist globally in time if

$$\|u_0\|_{L^{N/2}(\mathbb{R}^N)}$$

is sufficiently small. On the other hand, they proved that the solution blows up in finite time if

$$\left(\int_{\mathbb{R}^N} |x|^2 u_0 dx \right)^{N-2} < C \|u_0\|_{L^1(\mathbb{R}^N)}^N$$

for a sufficiently small constant C .

For the full parabolic-parabolic system (7) (the model considered in the present paper) and a smoothly bounded domain Ω in \mathbb{R}^3 , Boy [10] showed that there exists a unique solution of (7) locally in time for sufficiently smooth initial data compatible with the boundary data. Furthermore, for all $T > 0$ there exists a constant C_T , such that if the initial data satisfy

$$\|c_0\|_{H^2(\Omega)} < C_T, \|u_0\|_{L^\infty(\Omega)} < C_T$$

and

$$\|\nabla u_0\|_{L^2(\Omega)} < C_T,$$

then the problem (7) has a unique solution on $[0, T] \times \Omega$.

Horstmann and Winkler [38] proved that there exist initial data such that the corresponding solution of (7) blows up either in finite or in infinite time. A basic tool for their analysis was the Lyapunov functional introduced in [26, 53]:

$$F(u(t), c(t)) := \int_{\Omega} \frac{1}{2\chi} |\nabla c(t)|^2 + \frac{1}{2\chi} c^2(t) + u(t) \log(u(t)) - u(t)c(t) dx. \quad (10)$$

Similarly to their result for the parabolic-elliptic situation, Corrias and Perthame [20] showed that if $\Omega = \mathbb{R}^N$ and the initial data are such that

$$u_0 \in L^q(\mathbb{R}^N) \text{ with } q > N/2 \text{ and } \nabla c_0 \in L^N(\mathbb{R}^N)$$

are sufficiently small, then there exist solutions of (7) globally in time, and these solutions behave like those of the heat equation.

In a recent paper, Calvez, Corrias and Ebde [14] also analyzed the classical Keller-Segel system in \mathbb{R}^N , $N \geq 3$. In this reference, the authors try to describe (as far as possible) the dynamics in both situations: in the parabolic-elliptic case and in the fully parabolic case. Their main results for the former case and $\Omega = \mathbb{R}^N$ are: local existence without smallness assumption on the initial density, global existence

under an improved smallness condition, and a comparison of blow-up criteria. For the parabolic-parabolic case (7), they formulate criteria of the concentration phenomenon. Furthermore, they present a visualization tool based on a reduction of the parabolic-elliptic system to a finite-dimensional dynamical system of gradient flow type sharing some common features with the infinite-dimensional system.

As already mentioned above, the global existence of solutions to (9) is well known, and a proof is easy to construct. Therefore, we leave this as an exercise for the interested reader. In essence, the difference in the time asymptotic behavior of our two models (7) and (9) is caused by the way in which the production of the chemoattractant is handled. While model (7) assumes that the production of the chemoattractant is proportional to the cell density of the motile species, model (9) takes the saturating effect in the chemoattractant production into account. This effect can be interpreted as an alternative way to model quorum sensing effects in chemotaxis, which has also been proposed already in [54]. In view of the chemoattractant production, Nanjundiah wrote the following (see [54, p. 68]):

“At high cell-densities, one can expect a fall-off in the rate proportional (say) to the number of cell-pairs in a region: then $g(u, c) = g_0(c)u - g_1(c)u^2$. Similarly, one can expect a fall-off at high c .”

We will not go into further detail on this aspect since this would be a topic for a paper on its own. However, we wish to point out that the question as to how quorum sensing effects are modeled seems to have more than just one answer.

From the pattern forming point of view in chemotaxis one of the typical experiments with *Escherichia coli* bacteria done by J. Adler in 1966 has been quoted in [61]. To give the reader an illustration of the experimental setting we cite the following description from [61]:

*“About a million motile cells of *E. coli* are placed at one end of a capillary tube filled with a solution containing 2.5×10^{-4} molar galactose as the energy source, and the ends of the tube are closed with plugs of agar and clay.... The galactose is present in excess over the oxygen, since the concentration of oxygen in water saturated with air at 37°C is about 2.0×10^{-4} mole/l and it takes six molecules of oxygen to fully oxidize a molecule of galactose.... Soon afterward, two sharp, easily visible bands of bacteria have moved out from the origin, and some bacteria remain at the origin.”*

As a conclusion of these observations Adler stated that

“...the bacteria create a gradient of oxygen or of an energy source, and then they move preferentially in the direction of the higher concentration of the chemical. As a consequence, bands of bacteria ... form and move out.”

In other experiments with *E. coli*, Budrene and Berg [11] observed complex two-dimensional spots or stripe patterns that were caused by the interplay of diffusion, growth, and aggregation in response to the gradients of the chemoattractant. To analyze such spatial pattern formations, Mimura and Tsujikawa proposed in [48] chemotaxis models that include (8). To show that model (8) can describe the observed patterns, several scientists analyzed this model under some appropriate scaling. For example, Nadin, Perthame and Ryzhik [50] proved the existence of traveling wave solutions to a one-dimensional parabolic-elliptic version of (8) if the growth term is either a Fisher/KPP type or is truncated for small population densities. Their analysis provides $H_0^1(\mathbb{R})$ estimates, as well as some stability conditions on the coefficients which enforce an upper bound on the solution.

As mentioned above, solutions of model (8) exist globally in time due to the presence of the decay part $-u^2$ of the growth term $f(u)$. Tello and Winkler [66] considered more general forms of the growth term $f(u)$ for various spatial dimensions. Under some technical assumptions, they showed that there exists at least one global weak solution (compare [66, Theorem 3.3]) for arbitrary initial data. In our case, one can apply their result in [66, Theorem 2.5] that guarantees the existence of an unique global bounded classical solution for any initial data.

3 Numerical method

3.1 Galerkin discretization

In the numerical implementation, we solve equations (1) and (2) in a segregated fashion. In each time step, the transport equation for the chemoattractant concentration $c(t, \mathbf{x})$ is solved prior to that for the cell density $u(t, \mathbf{x})$. To begin with, both equations are written in the Galerkin weak form and discretized in space using (conforming) trilinear finite elements. The discretization in time is performed by the unconditionally stable implicit Euler method. The Crank-Nicolson or fractional-step- θ time-stepping schemes can be implemented in a similar way.

The system of linearized algebraic equations consists of two decoupled subproblems for the new vectors of discrete nodal values u^{n+1} and c^{n+1}

$$[\mathbf{M}(1) + \Delta t \mathbf{L}(D^n) - \Delta t \mathbf{K}(c^n)] u^{n+1} = \mathbf{M}(1)u^n + \Delta t \mathbf{q}^n, \quad (11)$$

$$[\mathbf{M}(1) + \Delta t \mathbf{L}(d) + \Delta t \mathbf{M}(s^n)] c^{n+1} = \mathbf{M}(1)c^n + \Delta t \mathbf{M}(g^n)u^n, \quad (12)$$

where $\mathbf{M}(\cdot)$ denotes the (consistent) mass matrix, $\mathbf{L}(\cdot)$ is a discrete diffusion operator, and $\mathbf{K}(c)$ is a discrete transport operator due to the chemotactic flux $A(u)B(c)C(\nabla c)$. For brevity, we use the abbreviations $D^n = D(u^n)$, $s^n = s(u^n)$, and $g^n = g(u^n)$. The entries of $\mathbf{M}(\cdot)$, $\mathbf{L}(\cdot)$, $\mathbf{K}(c)$ and \mathbf{q}^n are defined by

$$m_{ij}(\psi) = \int_{\Omega} \varphi_i \varphi_j \psi \, d\mathbf{x}, \quad \psi \in \{1, s(u), g(u)\}, \quad (13)$$

$$l_{ij}(\psi) = \int_{\Omega} \nabla \varphi_i \cdot \nabla \varphi_j \psi \, d\mathbf{x}, \quad \psi \in \{D(u), d\}, \quad (14)$$

$$k_{ij}(c) = \int_{\Omega} \nabla \varphi_i \cdot A(\varphi_j) B(c) C(\nabla c) \, d\mathbf{x}, \quad (15)$$

$$q_i^n = \int_{\Omega} \varphi_i q_j(u^n) \, d\mathbf{x}, \quad (16)$$

where φ_i is the finite element basis function associated with a vertex \mathbf{x}_i . In formula (15), the discontinuous concentration gradient ∇c can be replaced by a superconvergent approximation obtained using a suitable reconstruction technique (see, e.g., [73]).

3.2 Positivity preservation

The numerical behavior of the cell density u depends on the properties of the matrix $\mathbf{A} = \mathbf{M} + \Delta t(\mathbf{L} - \mathbf{K})$ that appears in the left-hand side of (11). Here and below, we suppress the explicit dependencies of the matrices when they can be easily deduced from the context, e.g., we write $\mathbf{M} = \mathbf{M}(1)$, $\mathbf{L} = \mathbf{L}(D^n)$ and $\mathbf{K} = \mathbf{K}(c^n)$ (the single matrix entries are treated in the same way). Sufficient conditions of positivity preservation are given by the following theorem.

Theorem 3.1 *If $\mathbf{A} = \{a_{ij}\}$ is an irreducibly diagonally dominant $n \times n$ matrix with $a_{ii} > 0$ for all $i = 1, \dots, n$ and $a_{ij} \leq 0$ for all $i \neq j$, then $\mathbf{A}^{-1} \geq 0$.*

Here and below, matrix/vector inequalities are meant to hold componentwise. For a proof of this theorem, we refer to the classical work by Varga ([70], p. 85).

Theorem 3.2 *Under the conditions of Theorem 3.1, the Galerkin scheme (11) is positivity-preserving, i.e., $u^n \geq 0, q^n \geq 0 \Rightarrow u^{n+1} \geq 0$.*

The proof of this result is very simple. In the case of linear or multilinear finite elements, we have $\mathbf{M} \geq 0$. Hence, the right-hand side $b^n = \mathbf{M}u^n + \Delta tq^n$ is nonnegative, and so is $u^{n+1} = \mathbf{A}^{-1}b^n$ by Theorem 3.1. \square

In general, the standard Galerkin approximation (11) does not satisfy the above constraints. The entries of the discrete diffusion operator \mathbf{L} have the right sign under rather mild assumptions on the geometric properties of the mesh (no sharp angles, moderate aspect ratios). However, some off-diagonal entries of $\mathbf{M} + \Delta t(\mathbf{L} - \mathbf{K})$ are strictly positive. If $m_{ij} + \Delta t(l_{ij} - k_{ij}) > 0$ for some $j \neq i$, then the conditions of Theorem 3.1 are violated, and the cell density u may become negative.

As shown by Kuzmin *et al.* [43, 44], the positivity constraint can be readily enforced at the discrete level using a conservative manipulation of the matrices $\mathbf{M}(1)$ and $\mathbf{K}(u^n, c^n)$. The former is approximated by its diagonal counterpart

$$\mathbf{M}_L := \text{diag}\{m_i\}, \quad m_i = \sum_j m_{ij}. \quad (17)$$

To satisfy sufficient DMP conditions, all negative off-diagonal entries of \mathbf{K} are eliminated by adding an artificial diffusion operator \mathbf{D} [43, 44]. For conservation reasons, this must be a symmetric matrix with zero row and column sums. For any pair of neighboring nodes i and j , the off-diagonal entry d_{ij} is defined as

$$d_{ij} = \max\{-k_{ij}, 0, -k_{ji}\}, \quad j \neq i. \quad (18)$$

Note that $d_{ji} = d_{ij}$ so that \mathbf{D} is symmetric, as desired. The diagonal coefficients d_{ii} are defined so that the row and column sums of \mathbf{D} are equal to zero

$$d_{ii} = - \sum_{j \neq i} d_{ij}. \quad (19)$$

The result is a positivity-preserving discretization of low order. It does not produce undershoots or overshoots but the inherent numerical diffusion smears the solution profiles. To rectify this, we apply a limited amount of compensating antidiffusion which is guaranteed to be local extremum diminishing (LED).

3.3 Flux limiting

By construction, the net artificial diffusion received by node i can be written as

$$(\mathbf{D}u)_i = \sum_j d_{ij}u_j = \sum_{j \neq i} d_{ij}(u_j - u_i) = - \sum_{j \neq i} f_{ij}, \quad (20)$$

where $f_{ij} = d_{ij}(u_i - u_j)$ is the antidiffusive flux from node j into node i . Inserting the so-defined fluxes into the right-hand side of the low-order scheme, we can remove artificial diffusion in smooth regions, where negative off-diagonal entries of \mathbf{K} do not pose any threat to positivity. In other regions, the magnitude of f_{ij} needs to be limited. In this paper, we use an upwind-biased limiting strategy [43] based on a generalization of the fully multidimensional flux-corrected transport (FCT) algorithm [72] and 1D total variation diminishing (TVD) schemes. The sums of fluxes that may violate the positivity constraint for node i are given by

$$P_i^\pm = \sum_{k_{ij} \leq k_{ji}} \max_{\min} \{0, f_{ij}\}. \quad (21)$$

The off-diagonal entries l_{ij} of the low-order operator $\mathbf{L} = \mathbf{K} + \mathbf{D}$ are nonnegative and define the upper/lower bounds for the FEM-TVD scheme as follows [43]

$$Q_i^\pm = \sum_{j \neq i} l_{ij} \max_{\min} (u_j - u_i). \quad (22)$$

Given a pair of nodes i and j with $k_{ij} < k_{ji}$, the raw antidiffusive fluxes f_{ij} and f_{ji} are multiplied by the common correction factor

$$\alpha_{ij} = \begin{cases} \min\{1, Q_i^+/P_i^+\}, & \text{if } f_{ij} > 0, \\ \min\{1, Q_i^-/P_i^-\}, & \text{otherwise} \end{cases} \quad (23)$$

and inserted into the right-hand side of the low-order system. This yields a nonlinear high-resolution finite element scheme satisfying the discrete maximum principle. For a detailed presentation of the underlying theory and practical implementation details (data structures, iterative solvers), we refer to Kuzmin [43].

4 Numerical results

4.1 Chemotaxis in a 3D chemostat

To consider some realistic settings for chemotactic movement in three spatial dimensions, we perform our numerical simulations in chemostat-like domains. A

chemostat (from **C**hemical environment is **s**tatic) is a popular bioreactor. The classical example is a cylindrical container to which a fresh medium is continuously added, while a culture liquid is continuously removed to keep the culture volume constant. This method is often used to cultivate certain species that are later used for some experimental observations. A major advantage of such bioreactors is the possibility to control the growth rate of the cultivated microorganism by changing the rate at which the medium is added. On the other hand, chemostats can also be used experimentally to observe the influence of external signals upon the motion of motile species or to monitor predator-prey interactions of species. For example, the effect of competition and chemotaxis between n -populations has been studied analytically by Kuiper in [42] and Le & Smith in [45]. Numerical simulations for multi-species chemotaxis models in three spatial dimensions will be considered in a forthcoming paper. Here we study the single species case.

We assume that the medium in the chemostat is static. By this we neglect the transport of u with the velocity of the fluid and concentrate on the chemotaxis-driven reactions only. The purpose of the following numerical experiments is to investigate the transport and blow-up behavior of the ‘cultural liquid’ and the applicability of the FEM-TVD algorithm to chemotaxis models in the three-dimensional space. Also for simplicity, we do not take into account the continuous ‘feed’ of chemoattractants and cell-‘effluent’.

We consider the minimal Keller-Segel chemotaxis model

$$u_t = \Delta u - \chi \nabla \cdot (u \nabla c), \quad (24)$$

$$c_t = \Delta c - c + u, \quad (25)$$

which is obtained from the system (1)–(2) by setting

$$\begin{aligned} A(u) &= u, & B(c) &= \chi, & C(\nabla c) &= \nabla c, & D(u) &= 1, & q(u) &= 0, \\ d &= 1, & s(u) &= 1, & g(u) &= 1. \end{aligned}$$

The homogeneous natural boundary conditions (or ‘total flux’ boundary conditions for u and c)

$$\mathbf{n} \cdot (\nabla u - u \nabla c) = \mathbf{n} \cdot \nabla c = 0 \quad \text{on } \partial\Omega \quad (26)$$

and the following initial data

$$u(0, \mathbf{x}) = 1000 \cdot e^{-100 \cdot (x_1^2 + x_2^2 + (x_3 - 2)^2)} \quad \text{in } \Omega, \quad (27)$$

$$c(0, \mathbf{x}) = 500 \cdot e^{-50 \cdot (x_1^2 + x_2^2 + (x_3 - 3)^2)} \quad \text{in } \Omega \quad (28)$$

are prescribed. Inoculum of chemoattractant and cells according to (27)–(28) is shown in Figure 1(a).

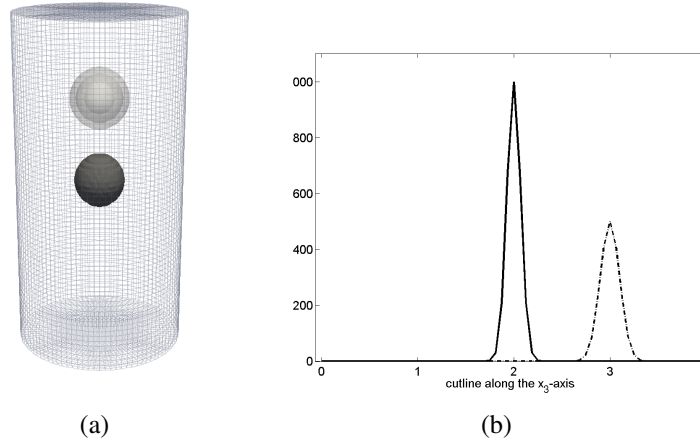


Figure 1: (a) Initial conditions for the cells (dark spot) and the chemoattractant (grey spot); (b) cutlines of the cell distribution (solid line) and chemoattractant concentration (dashed line) along the x_3 -axis.

The stability of the system is heavily dependent on the chemoattractive sensitivity χ . By fixing all involved parameters and varying the magnitude of χ one can make either the diffusion processes or the chemoattractive transport of cells dominant. The former situation leads to steady-state solutions, whereas the latter gives rise to evolving in time solutions, blow-ups etc.

In Figures 2–4, we examine the distribution of cells and of the chemoattractant for the chemotaxis sensitivities $\chi = 1$, $\chi = 2$, and $\chi = 3$, respectively. One can observe that for smaller χ the propagation of cells into the region with high concentrations of the chemoattractant is relatively slow. In this case, the diffusion of cells is more pronounced than the chemoattractive transport. For larger χ , the propagation of cells into the region of high chemoattractant concentrations is accelerated. The magnitude of u increases rapidly, and a blow-up occurs.

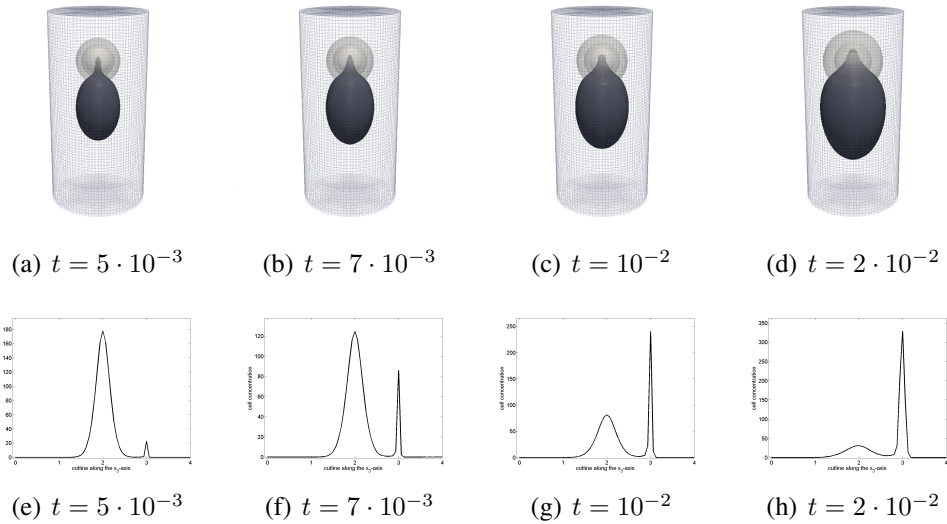


Figure 2: Development of cell and chemoattractant concentrations for $\chi = 1$ at $t = 5 \cdot 10^{-3}, 7 \cdot 10^{-3}, 10^{-2}, 2 \cdot 10^{-2}$; $\Delta t = 10^{-4}$. **Top:** Distribution of cells u (red) and chemoattractant c (green). **Bottom:** Cutline along the x_3 -axis for cells u .

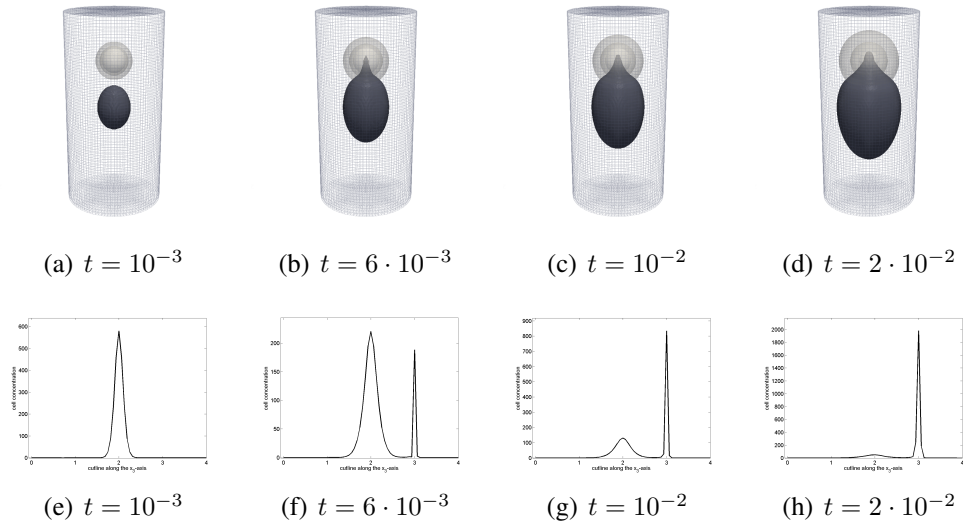


Figure 3: Development of cell and chemoattractant concentrations for $\chi = 2$ at $t = 10^{-3}, 6 \cdot 10^{-3}, 10^{-2}, 2 \cdot 10^{-2}$; $\Delta t = 10^{-4}$. **Top:** Distribution of cells u (red) and chemoattractant c (green). **Bottom:** Cutline along the x_3 -axis for cells u .

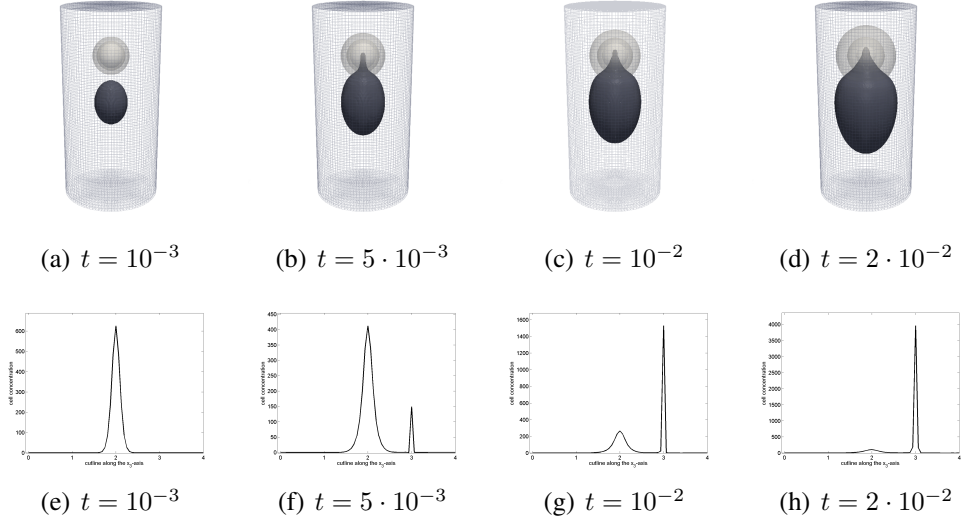


Figure 4: Development of cell and chemoattractant concentrations for $\chi = 3$ at $t = 10^{-3}, 5 \cdot 10^{-3}, 10^{-2}, 2 \cdot 10^{-2}$; $\Delta t = 10^{-4}$. **Top:** Distribution of cells u (red) and chemoattractant c (green). **Bottom:** Cutline along the x_3 -axis for cells u .

Figures 2(h), 3(h) and 4(h) display snapshots of the numerical solution at late time instants which represent the crucial part of the simulation process. Here we observe a strong aggregation of the cell density, which produces a peak at the point $(0, 0, 3)^T$. The proposed FEM-TVD method delivers smooth, positivity preserving and nonoscillatory profiles of the cell distribution u and chemoattractant concentration c alike. At the same time, the pure Galerkin scheme without any stabilization technique is incapable of delivering a plausible solution: non-physical negative values in the cell density grow rapidly as time evolves, which leads to an abnormal termination of the simulation run (see Figures 5(a)-5(c)). The chemoattractant concentration c calculated with the unconstrained Galerkin scheme also exhibits spurious oscillations (albeit with a smaller amplitude and, obviously, with a small delay in time). The plots of this oscillatory solution are not presented since they do not carry any additional information.

Local mesh refinement can significantly improve the accuracy of a finite element approximation. Numerical experiments indicate that the use of mesh adaptation is particularly important for blow-up problems and problems with strong localization effects. This is a very broad topic which is beyond the scope of the present paper. The interested reader is referred to [64] for some results illustrating the

benefits of mesh adaptation in the context of a two-dimensional blow-up problem.

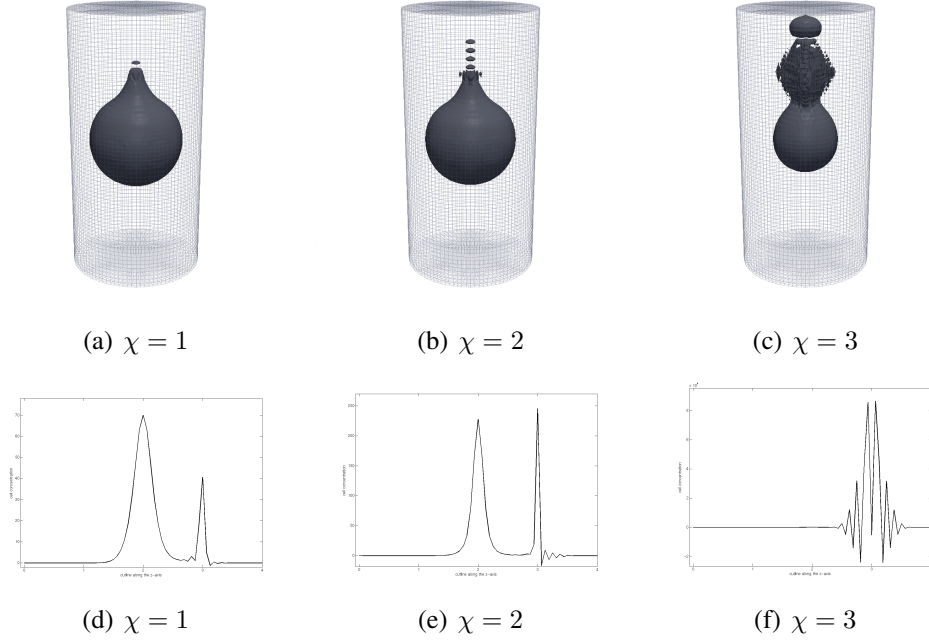


Figure 5: The pure Galerkin scheme, cell densities for $\chi = 1, 2$ and 3 at time $t = 2 \cdot 10^{-2}$. **Top:** Oscillatory distribution of cells. **Bottom:** Cutline along the x_3 -axis for cells u .

4.2 Pattern formation

In the next example, we use our high-resolution FEM-TVD method to simulate the pattern dynamics of motile cells *Escherichia coli*. Several chemotaxis models describing this phenomenon can be found in the literature. In this numerical study, we adopt the one proposed by Aida *et al.* [4] and replace the commonly employed cubic growth rate by the classical Fisher-type model,

$$u_t = d_u \Delta u - \chi \nabla \cdot (u \nabla c) + u(1 - u), \quad (29)$$

$$c_t = \Delta c - \beta c + u. \quad (30)$$

System (29)–(30) can be obtained from the general form of the chemotaxis problem (1)–(2) by setting

$$A(u) = u, \quad B(c) = \chi, \quad C(\nabla c) = \nabla c, \quad D(u) = d_u, \quad q(u) = u(1 - u), \\ d = 1, \quad s(u) = \beta, \quad g(u) = 1.$$

As before, we prescribe homogeneous natural boundary conditions on $\partial\Omega$. The initial conditions for this test are given by

$$u(0, \mathbf{x}) = 1 + \sigma(\mathbf{x}), \\ c(0, \mathbf{x}) = 1/32,$$

where $\sigma(\mathbf{x})$ is a small perturbation defined as

$$\sigma(\mathbf{x}) = \begin{cases} \text{random}[0, 1], & \text{if } \|\mathbf{x}\|_2 \leq \sqrt{2}, \\ 0, & \text{otherwise.} \end{cases}$$

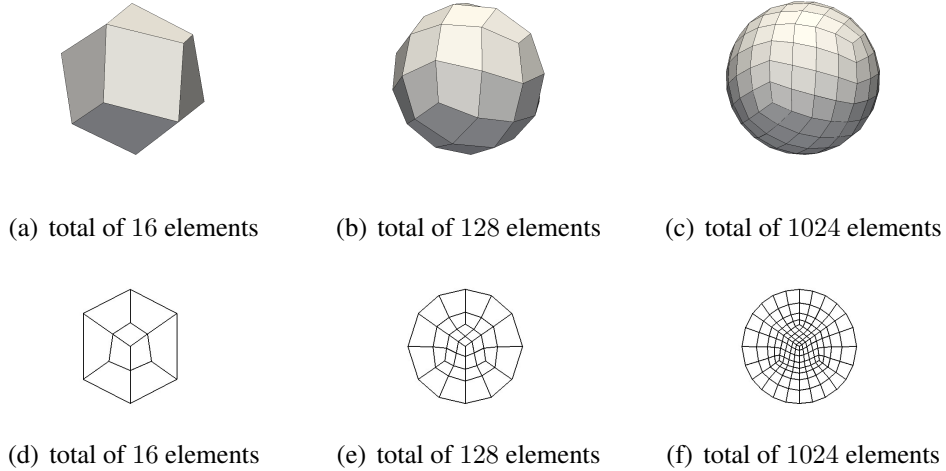


Figure 6: Spherical mesh for three successive refinement levels. **Top:** Three-dimensional visualization. **Bottom:** Two-dimensional cutplane along the x_1x_2 -plane.

Following [4], we choose the following parameter settings: $d_u = 0.0625$, $\chi = 8.5$, and $\beta = 32$. Numerical simulations are performed in the sphere $\|\mathbf{x}\|_2 \leq 8$ which

is discretized using an *almost* uniform mesh which is considerably finer than the one shown in figures 6(c) and 6(f) (resulting in 4,194,304 conforming trilinear finite elements). The time step is taken to be $\Delta t = 0.1$.

We have already reported in [64] that 2D solutions of (29)–(30) are very sensitive to the choice of parameters, such as χ , σ , etc. The same effect is observed during numerical experiments in 3D. Figure 7 displays the bacteria distribution calculated with the FEM-TVD algorithm. Placed in the center, the initial concentration of bacteria propagates into the whole domain in a moving-wave pattern. Advancing wave-fronts leave trailing spikes in response to the chemosensitivity.

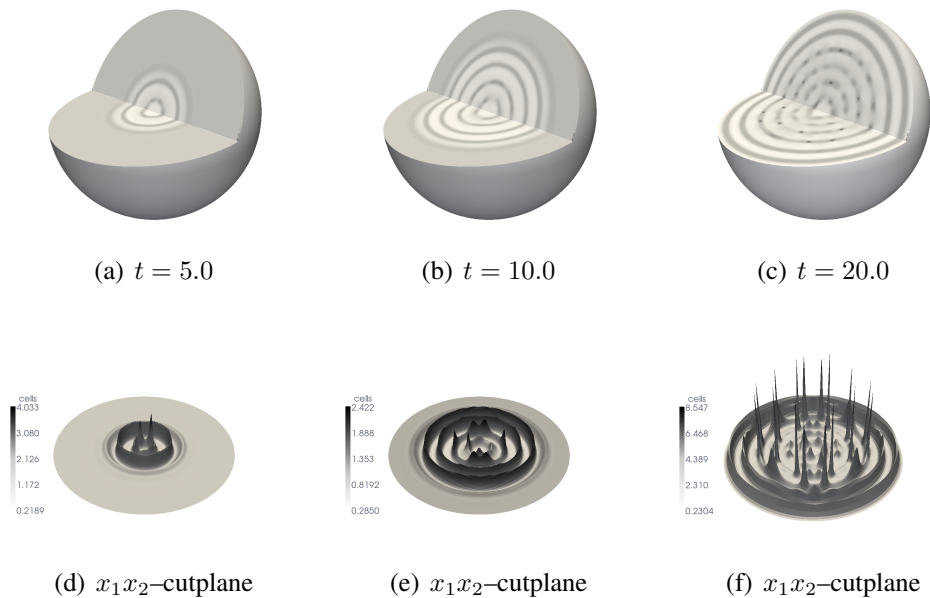


Figure 7: Pattern formation simulated with the FEM-TVD algorithm. The screenshots were taken at times $t = 5.0, 10.0, 20.0$.

4.3 Aggregation of bacteria

As last example for our 3D simulations, we consider the chemotaxis model proposed by Tyson *et al.* in [67] (see also [68] and [69])

$$u_t = d_u \Delta u - \chi \nabla \cdot \left[\frac{u}{(1+c)^2} \nabla c \right], \quad (31)$$

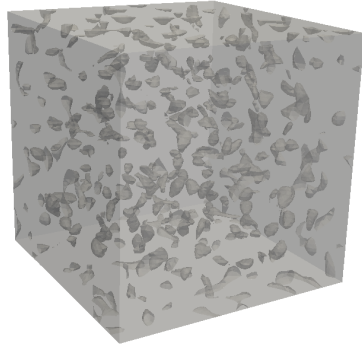
$$c_t = d_c \Delta c - c + w \frac{u^2}{\mu + u^2}. \quad (32)$$

System (31)–(32) describes an aggregating behavior of the bacteria *Escherichia coli* and *Salmonella typhimurium*. It can readily be seen that this system is of the form (29)–(30) and, therefore, can be solved using the FEM-TVD algorithm.

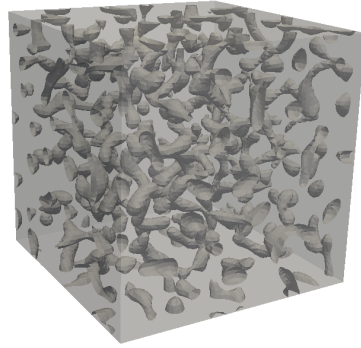
As usual, we prescribe the homogeneous natural boundary conditions on $\partial\Omega$. The initial conditions are chosen to be

$$\begin{aligned} u(0, \mathbf{x}) &= 0.9 + 0.2 \sigma(\mathbf{x}), \\ c(0, \mathbf{x}) &= 0, \end{aligned}$$

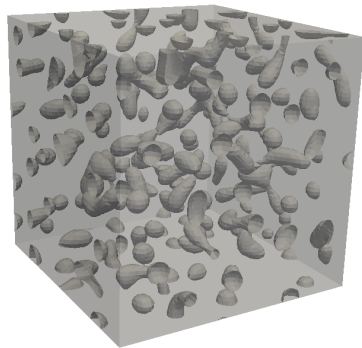
where $\sigma(\mathbf{x}) = \text{random}[0, 1]$ in Ω . Numerical simulations are performed in the cubic domain $\Omega = [0, 16]^3$. A uniform mesh with $h = 1/4$ and a total of 262,144 trilinear elements is employed. The time step is taken to be $\Delta t = 0.01$. Other parameters are chosen as follows: $d_u = 1$, $d_c = 0.33$, $\chi = 80$, $w = 1$. Numerical results at a sequence of consecutive time points are shown in Figures 8(a)–8(d). Randomly distributed bacteria aggregate into *cylindrical capsules*. As time evolves, the concentration of bacteria in these capsules grows, and the distances between the capsules increase. The proposed FEM-TVD algorithm keeps u non-negative and yields an accurate resolution of concentration points. Flux correction makes it more reliable than the underlying Galerkin method and less diffusive than the corresponding low-order scheme.



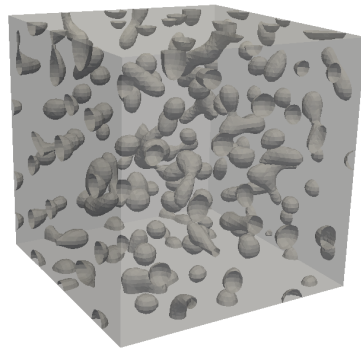
(a) $t = 1.0$



(b) $t = 2.0$



(c) $t = 4.0$



(d) $t = 5.0$

Figure 8: Aggregation of bacteria. The screenshots were taken at the distinct times $t = 1.0, 2.0, 4.0, 5.0$.

5 Conclusions

A theoretical and numerical framework for solving 3D chemotaxis problems was developed and analyzed. The proposed FEM-TVD algorithm preserves the positivity of cell densities and yields a crisp resolution of steep gradients. The presented methodology is well suited for numerical experiments that demonstrate chemotactical response of motile species in a bio-container. For example, the

developed code can be used as a tool to study the competition between self-organization and attraction to an external source in more detail. Furthermore, it is capable of reproducing the classical experiments of Adler [1, 2] and his group in the context of computer simulations. The computational approach gives an additional insight into the mechanisms behind pattern formation of traveling bands in chemotaxis systems.

Application to system (8) indicates that our numerical scheme is a viable tool for simulating the growth of bacterial colonies. In general, this growth is driven by several complex biomechanical processes, creating the rich variety of shapes that are exhibited by the colonies. For example, the division and motion of cells can cause formation and propagation of unstable fronts. This gives rise to various patterns, such as spiral waves [47], aggregates [49] and dendrites [9, 27]. The presented algorithm makes it possible to gain deeper insight into these pattern formation processes, thus helping modelers and analysts to understand the underlying biological mechanisms in more detail.

From the analytical point of view, the proposed numerical framework can be used to investigate the blow-up behavior of solutions to the so-called classical chemotaxis model (7) in three space dimensions. In particular, one can think of using a computational study to find qualitative criteria for identifying initial data that lead to finite blow-up or to globally existing solution in 3D. The existence of such initial data has been shown in [20]. The new criteria might give some hints for finding an alternative blow-up proof instead of using the “usual” second momentum method, the only tool which is currently available for proving the finite time blow-up for certain initial data in 3D.

As a final note, we would like to point out some promising directions for further investigations. First of all, the current implementation of the FEM-TVD scheme requires mass lumping. Work is under way to implement a new slope limiter for the consistent mass matrix and convection/diffusion operators. This will provide a further gain of accuracy for strongly time-dependent problems. Furthermore, the numerical study presented in this paper should be extended to complex chemotaxis systems with multiple populations and chemoactive substances. The numerical treatment of particularly sensitive applications may require further improvements of the FEM-TVD algorithm. In particular, flux limiting may need to be performed using a suitable synchronization of correction factors in the presence of multiple “unstable” entities, e.g., in the case of chemotaxis problems that involve simulta-

neous transport of more than one species. These applications and improvements warrant further research to be presented in a forthcoming paper.

Acknowledgements

This research was supported by the German Research Association (DFG) under Grant KU 1530/3-2. Robert Strehl is also supported by a scholarship of the TU Dortmund.

References

- [1] J. ADLER, *Chemotaxis in bacteria*, Science. **153** (1966), no. 3737, pp. 708–716.
- [2] J. ADLER, *Chemotaxis in bacteria*, Ann. Rev. Biochem. **44** (1975), pp. 341–356.
- [3] M. AIDA AND A. YAGI, *Target pattern solutions for chemotaxis-growth system*, Scientiae Mathematicae Japonicae **59** (2004), no. 3, pp. 577–590.
- [4] M. AIDA, T. TSUJIKAWA, M. EFENDIEV, A. YAGI AND M. MIMURA, *Lower estimate of the attractor dimension for a chemotaxis growth system*, J. London Math. Soc. **74** (2006), no. 2, pp. 453–474.
- [5] H. AMANN, *Dynamic theory of quasilinear parabolic equations II. Reaction-Diffusion Systems*, Differential and Integral Eqns. **3** (1990), pp. 13–75.
- [6] H. AMANN, *Nonhomogeneous linear and quasilinear elliptic and parabolic boundary value problems*, Function Spaces, Differential Operators and Nonlinear Analysis (Eds. Schmeisser, Triebel), Teubner Texte zur Mathematik **133** (1993), pp. 9–126.
- [7] D. AMBROSI, F. BUSSOLINO AND L. PREZIOSI, *A review of vasculogenesis models*, Computational and Mathematical Methods in Medicine **6** (2005), no. 1, 1–19.
- [8] A. R. A. ANDERSON, M. A. J. CHAPLAIN, E. L. NEWMAN, R. J. C. STEELE AND A. M. THOMPSON, *Mathematical modelling of tumour invasion and metastasis*, Journal of Theoretical Medicine **2** (1999), pp. 129–154.

- [9] E. BEN-JACOB, I. COHEN, I. GOLDING AND Y. KOZLOVSKY, *Modeling branching and chiral colonial patterning of lubricating bacteria*, in: Mathematical models for biological pattern formation, IMA Vol. Math. Appl., Springer, New York **121** (2001), pp. 211–253.
- [10] A. BOY, *Analysis for a system of coupled reaction-diffusion parabolic equations arising in biology*. Computers Math. Applic **32** (1996), pp. 15–21.
- [11] E. O. BUDRENE AND H. C. BERG, *Complex patterns formed by motile cells of Escherichia coli*, Nature **349** (1991), pp. 630–633.
- [12] E. O. BUDRENE AND H. C. BERG, *Dynamics of formation of symmetrical patterns by chemotactic bacteria*, Nature **376** (1995), no. 6535, pp. 49–53.
- [13] M. BURGER, M. DI FRANCESCO AND Y. DOLAK-STRUSS, *The Keller-Segel model for chemotaxis with prevention of overcrowding: Linear vs. nonlinear diffusion*, SIAM J. Math. Anal. **38** (2006), pp. 1288–1315.
- [14] V. CALVEZ, L. CORRIAS AND M. A. EBDE, *Blow-up, concentration phenomenon and global existence for the Keller-Segel model in high dimension*, Preprint arXiv:1003.4182v1 (2010).
- [15] M. A. J. CHAPLAIN AND A. M. STUART, *A model mechanism for the chemotactic response of endothelial cells to tumour angiogenesis factor*, IMA Journal of Mathematics Applied in Medicine and Biology **10** (1993), pp. 149–168.
- [16] A. CHAUVIERE, T. HILLEN AND L. PREZIOSI, *Modeling cell movement in anisotropic and heterogeneous network tissues*, Networks and heterogeneous media **2** (2007), no. 2, pp. 333–357.
- [17] A. CHERTOCK AND A. KURGANOV, *A second-order positivity preserving central-upwind scheme for chemotaxis and haptotaxis models*, Numer. Math. **111** (2008), pp. 169–205.
- [18] S. CHILDRESS, *Chemotactic collapse in two dimensions*, Lecture Notes in Biomathematics, Springer-Verlag **55** (1984), pp. 61–66.
- [19] S. CHILDRESS AND J.K. PERCUS, *Nonlinear aspects of chemotaxis*, Math. Biosc. **56** (1981), pp. 217–237.

- [20] L. CORRIAS AND B. PERTHAME, *Asymptotic decay for the solutions of the parabolic-parabolic Keller-Segel chemotaxis system in critical spaces*. Mathematical and Computer Modelling **47** (2008), pp. 755–764.
- [21] L. CORRIAS, B. PERTHAME AND H. ZAAG, *Global solutions of some chemotaxis and angiogenesis systems in high space dimensions*. Milan J. Math. **72** (2004), pp. 1–28.
- [22] Y. DOLAK AND C. SCHMEISER, *The Keller-Segel model with logistic sensitivity function and small diffusivity*, SIAM J. Appl. Math. **66** (2005), pp. 595–615.
- [23] Y. EPSHTEYN, *Discontinuous Galerkin methods for the chemotaxis and haptotaxis models*, J. Comput. Appl. Math. **224** (2009), no. 1, pp. 168–181.
- [24] Y. EPSHTEYN AND A. KURGANOV, *New interior penalty discontinuous Galerkin methods for the Keller-Segel chemotaxis model*, SIAM J. Numer. Anal. **47** (2008), no. 1, pp. 386–408.
- [25] F. FILBET, *A finite volume scheme for the Patlak-Keller-Segel chemotaxis model*, Numer. Math. **104** (2006), no. 4, 457–488.
- [26] H. GAJEWSKI AND K. ZACHARIAS, *Global behavior of a reaction-diffusion system modelling chemotaxis*, Math. Nachr. **195** (1998), pp. 77–114.
- [27] I. GOLDING, Y. KOZLOVSKY, I. COHEN AND E. BEN-JACOB, *Studies of bacterial branching growth using reaction-diffusion models for colonial development*, Phys. A **260** (1998), pp. 510–554.
- [28] M. A. HERRERO, *Asymptotic properties of reaction-diffusion systems modelling chemotaxis*, Applied and industrial mathematics, Venice–2, 1998, Kluwer Acad. Publ., Dordrecht 2000, pp. 89–108.
- [29] M. A. HERRERO, E. MEDINA AND J. J. L. VELÁZQUEZ, *Finite-time aggregation into a single point in a reaction diffusion system*, Nonlinearity **10** (1997), pp. 1739–1754.
- [30] M. A. HERRERO, E. MEDINA AND J. J. L. VELÁZQUEZ, *Self-similar blow-up for a reaction diffusion system*, Journal of Computational and Applied Mathematics **97** (1998), pp. 99–119.

- [31] T. HILLEN, *M⁵ mesoscopic and macroscopic models for mesenchymal motion*, J. Math. Biol. **53** (2006), pp. 585–616.
- [32] D. HORSTMANN, *Lyapunov functions and L^p -estimates for a class of reaction-diffusion systems*, Colloquium Mathematicum **87** (2001), pp. 113–127.
- [33] D. HORSTMANN, *From 1970 until present: The Keller-Segel model in chemotaxis and its consequences I*, Jahresberichte der DMV **105** (2003), pp. 103–165.
- [34] D. HORSTMANN, *Generalizing Keller-Segel: Lyapunov functionals, steady state analysis and blow-up results for multi-species chemotaxis models in the presence of attraction and repulsion between competitive interacting species*, Journal of Nonlinear Sciences, to appear.
- [35] D. HORSTMANN AND M. LUCIA, *Nonlocal elliptic boundary value problems relate to chemotactic movement of mobile species*, RIMS Kôkyûroku Bessatsu B **15** (2009), pp. 39–72.
- [36] D. HORSTMANN AND M. LUCIA, *Uniqueness and symmetry of equilibria in a chemotaxis model*, Journal für die Reine und Angewandte Mathematik, to appear.
- [37] D. HORSTMANN AND G. WANG, *Blow-up in a chemotaxis model without symmetry assumptions*, European Journal of Applied Mathematics **12** (2001), pp. 159–177.
- [38] D. HORSTMANN AND M. WINKLER, *Boundedness vs. blow-up in a chemotaxis system*, Journal of Differential Equations **215** (2004), pp. 52–107.
- [39] A. JAMESON, *Analysis and design of numerical schemes for gas dynamics. I. Artificial diffusion, upwinding biasing, limiters and their effect on accuracy and multigrid convergence*, International Journal of Computational Fluid Dynamics **4** (1995), pp. 171–218.
- [40] E. F. KELLER AND E. F. SEGEL, *Initiation of slime mold aggregation viewed as an instability*, J. Theor. Biol. **26** (1970), pp. 399–415.
- [41] E. F. KELLER AND E. F. SEGEL, *Model for chemotaxis*, J. Theor. Biol. **30** (1971), pp. 225–234.

- [42] H. J. KUIPER, *A priori bounds and global existence for a strongly coupled quasilinear parabolic system modeling chemotaxis*, Electron. J. Differ. Equ. **2001** (2001), no.52, pp. 1–18.
- [43] D. KUZMIN, *On the design of general-purpose flux limiters for implicit FEM with a consistent mass matrix. I. Scalar convection.*, J. Comput. Phys. **219** (2006), pp. 513–531.
- [44] D. KUZMIN AND M. MÖLLER, *Algebraic flux correction I. Scalar conservation laws*, in: D. KUZMIN, R. LÖHNER, S. TUREK (eds), *Flux-Corrected Transport: Principles, Algorithms, and Applications*, Springer, Berlin (2005), pp. 155–206.
- [45] D. LE AND H. L. SMITH, *Steady states of models of microbial growth and competition with chemotaxis*, J. M. A. A. **229** (1999), pp. 295–318.
- [46] P. R. M. LYRA, K. MORGAN, J. PERAIRE AND J. PEIRO, *TVD algorithms for the solution of the compressible Euler equations on unstructured meshes*, International Journal for Numerical Methods in Fluids **19** (1994), pp. 827–847.
- [47] P. K. MAINI, *Applications of mathematical modelling to biological pattern formation*, in: D. REGUERA, L. L. BONILLA, J. M. RUBI (eds), *Coherent structures in complex systems*, Springer Lecture Notes in Phys., **567** (2001), pp. 205–217.
- [48] M. MIMURA AND T. TSUJIKAWA, *Aggregating pattern dynamics in a chemotaxis model including growth*, Physica A, **230** (1996), pp. 499–543.
- [49] J. D. MURRAY, *Mathematical biology II: Spatial models and biomedical applications*, vol. 18 of Interdisciplinary Applied Mathematics, Springer-Verlag, New York, third ed., 2003.
- [50] G. NADIN, B. PERTHAME AND L. RYZHIK, *Traveling waves for the Keller-Segel system with Fisher birth terms*, Interfaces and Free Boundaries, **10** (2008), pp. 517–538.
- [51] T. NAGAI, *Blow-up of radially symmetric solutions to a chemotaxis system*, Adv. Math. Sci. Appl. **5** (1995), pp. 581–601.

- [52] T. NAGAI, *Blowup of nonradial solutions to parabolic-elliptic systems modeling chemotaxis in two-dimensional domains*, J. Inequal. Appl. **6** (2001), pp. 37–55.
- [53] T. NAGAI, T. SENBA AND K. YOSHIDA, *Application of the Moser-Trudinger inequality to a parabolic system of chemotaxis*, Funkc. Ekvacioj, Ser.Int. **40** (1997), pp. 411–433.
- [54] V. NANJUNDIAH, *Chemotaxis, signal relaying and aggregation morphology*, J. Theor. Biol. **42** (1973), pp. 63–105.
- [55] K. OSAKI AND A. YAGI, *Finite dimensional attractors for one-dimensional Keller-Segel equations*. Funkcialaj Ekvacioj **44** (2001), pp. 441–469.
- [56] C. S. PATLAK, *Random walk with persistence and external bias*, Bull. Math. Biol. Biophys. **15** (1953), pp. 311–338.
- [57] B. PERTHAME, *Transport equations in biology*, Birkhäuser-Basel, Verlag, Switzerland, 2007.
- [58] A. B. POTAPOV, T. HILLEN, *Metastability in chemotaxis models*, J. Dyn. Diff. Eq. **17** (2005), pp. 293–330.
- [59] D. L. ROPP AND J. N. SHADID, *Stability of operator splitting methods for systems with indefinite operators: Advection-diffusion-reaction systems*, J. Comput. Phys. **228** (2009), no. 9, pp. 3508–3516.
- [60] N. SAITO, *Conservative upwind finite-element method for a simplified Keller-Segel system modelling chemotaxis*, IMA J. Numer. Anal., **27** (2007), pp. 332–365.
- [61] T. L. SCRIBNER, L. A. SEGEL AND E. H. ROGERS, *A numerical study of the formation and propagation of traveling bands of chemotactic bacteria*, J. Theor. Biol. **46** (1974), pp. 189–219.
- [62] T. SENBA AND T. SUZUKI, *Parabolic System of Chemotaxis: Blowup in a Finite and the Infinite Time*, Methods Appl. Anal. **8** (2001), pp. 349–368.
- [63] T. SENBA AND T. SUZUKI, *Applied Analysis*, Imperial College Press, 2004.

- [64] R. STREHL, A. SOKOLOV, D. KUZMIN AND S. TUREK, *A flux-corrected finite element method for chemotaxis problems*, CMAM **10** (2010), no. 2, pp. 118–131.
- [65] Y. TAO AND M. WANG, *A combined chemotaxis-haptotaxis system: the role of logistic source*, SIAM J. Math. Anal. **41** (2009), no. 4, pp. 1533–1558.
- [66] J. I. TELLO AND M. WINKLER, *A Chemotaxis System with Logistic Source*, Comm. Partial Diff. Eqns **32** (2007), pp. 849–877.
- [67] R. TYSON, S. R. LUBKIN AND J. D. MURRAY, *A minimal mechanism for bacterial pattern formation*, Proc. R. Soc. Lond. B **266** (1999), pp. 299–304.
- [68] R. TYSON, S. R. LUBKIN AND J. D. MURRAY, *Model and analysis of chemotactic bacterial patterns in a liquid medium*, J. Math. Biol. **38** (1999), pp. 359–375.
- [69] R. TYSON, L. G. STERN AND R. J. LEVEQUE, *Fractional step methods applied to a chemotaxis model*, J. Math. Biol. **41** (2000), pp. 455–475.
- [70] R. S. VARGA, *Matrix Iterative Analysis*. Prentice-Hall, Englewood Cliffs, 1962.
- [71] A. YAGI, *Norm behavior of solutions to a parabolic system of chemotaxis*, Math. Japonica **45** (1997), pp. 241 – 265.
- [72] S. T. ZALESK, *Fully multidimensional Flux-Corrected Transport algorithm for fluids*, Journal of Computational Physics **31** (1979), pp. 335–362.
- [73] O.C. ZIENKIEWICZ AND J.Z. ZHU, *The superconvergent patch recovery and a posteriori error estimates. Part 1: The recovery techniques*. Int. J. Numer. Methods Engrg. **33** (1992), pp. 1331–1364.